# OVERVIEW OF THE STATE-OF-THE-ART AND MOST PROMISING MEASUREMENT TECHNIQUES

by Prof. Martin Wegener, Prof. Nigel Johnson and Prof. Alex Schuchinsky, Prof. Constantin Simovski and Prof. Sergei Tretyakov.

(EU FP7 Contract No. 218696-ECONAM)

2010

# Contents

# 1 Introduction

Experimental characterisation of metamaterials is predominantly based upon the measurements of the scattering characteristics of the specimens illuminated by plane electromagnetic waves in optical, THz and microwave spectral ranges. Artificial nanostructured materials exhibit strong resonant response to electromagnetic frequencies in the optical part of the electromagnetic spectrum, thus, optical measurements are of prime interest for this overview. Here we discuss measurement techniques for experimental characterization of electromagnetic parameters of nanostructured materials, mainly in the optical part of the spectrum.

Before directly addressing the metamaterial characterization issues, it is necessary to remark that on the notion of the "optical wavelengths". In the literature it is not strictly defined, but in the bulk of the literature it is understood as the frequency region including infra-red, visible, and ultra-violet frequencies. This corresponds, roughly, to the range of frequencies from 3 THz to 30 PHz (PetaHertz=$10^{15}$ Hz). In terms of the wavelength, this is equivalent to the range from 0.1 mm to 10 nm. In general, "optical" refers to electromagnetic radiation that can be influenced by lenses and gratings. At lower frequencies, approaching the far-infrared (or the "THz regime"), the issues of sample characterization tend be somewhat different from the optical regime. At frequencies higher than the visible light, the required inhomogeneity scale becomes too small to be technologically feasible at present, and there are no artificial electromagnetic materials that would function at ultra-violet frequencies. The visible part of the optical spectrum is between approximately 400 THz (red) to 790 THz (blue) or from 390 nm (blue) to 760 nm (red).

Also it is instructive to briefly recall how today's state-of-the-art metamaterials at optical frequencies look like – as this aspect poses the relevant constraints to the characterization process. The vast majority of metamaterial structures have been made via serial, hence time-consuming, lithographic approaches (e.g., electron-beam lithography, focused-ion-beam lithography, or direct laser writing). As a result, typical sample footprints are only of the order of $100 \times 100$ $\mu$m$^2$. This limited sample size, with respect to the source and detector area at shorter wavelength of measurement leads to use of focusing lenses and the unavoidable averaging of the measurements. This is further discussed in Section 1.3. Rather recent brief [1, 2] and comprehensive [3] reviews of the corresponding magnetic and/or negative-index metamaterials can be found in the literature. Examples of notable exceptions are metamaterials made via holographic lithography [4, 5] or nano-imprint techniques [6]. The footprint of the latter specimens is of the order of square-centimetres. Yet much larger footprints can be realized along these lines in the future, and there are attempts to use some self-assembly techniques to fabricate metamaterial structures [7–9].

Furthermore, the vast majority of metamaterials at optical wavelengths demonstrated experimentally thus far contain only a single functional layer [1–3], which can contain more than one physical layer. Notable recent experimental exceptions are a three-functional-layer negative-index metamaterial at 1.4-$\mu$m wavelength [10], a four-functional-layer magnetic metamaterial at 3.7-$\mu$m wavelength [11], and a ten-functional-layer negative-index metamaterial at 1.8-$\mu$m wavelength [12]. All of these have a total thickness significantly less than one wavelength of light in free space. Interesting metal-insulator-metal slot

waveguide structures supporting backward waves over many wavelengths of light along the propagation direction in the waveguide plane have also been reported [13]. However, their optical characterization is not discussed here as such waveguides are not classified as "metamaterials". It is important to note that all the actually fabricated optical metamaterial structures published to date are anisotropic, often they are even biaxial and bi-anisotropic. These geometric variations in the metamaterial parameters further complicate the measurements and analysis effectively multiplying the problem by the number of unique directions in the metamaterial. Furthermore, essentially all metamaterial structures are mechanically supported by some kind of a dielectric substrate – an aspect, which has to be accounted for in the characterization process as well.

An EU sponsored publication [14] covers the basic electromagnetic theory and fabrication methods involved.

## 1.1 The ideal measurement

The conceptually perfect experiment on a periodic metamaterial with sub-wavelength lattice constant can provide measurements of nothing more than the frequency-dependent complex reflectance and transmittance of the sample for all incidence angles and polarizations of the impinging ideal monochromatic plane wave. Furthermore, this ideal measurement should comprise analysis of the (generally elliptical) polarization state of light scattered by the sample. Clearly, in linear optics, frequency-domain information can equivalently be expressed in the time-domain, where "complex" translates into amplitude and phase of the wave. For imperfect or for (intentionally) non-periodic metamaterial samples, also scattering of light into the entire solid angle (so called "diffuse scattering") can occur because any inhomogeneities scatter light in all directions. In the ideal experiment this scattering would also have to be characterized completely in an experiment for all solid angles.

Anything beyond this, e.g., retrieval of whatever effective optical parameters (refractive index, wave impedance, dielectric permittivity, magnetic permeability, bi-anisotropy parameters, etc.), is not subject of the experimental optical characterization process itself but it is subject of interpretation (!) of the acquired experimental data. This distinct step – which is closely related to and interlinked to the retrieval of these parameters through the theoretical models or numerical simulations – will be discussed in other parts of this overview. Non-linear metamaterials, for example those with gain, are not considered here.

## 1.2 Standard measurement techniques

Standard optical measurement techniques (which typically do not provide phase information) can be found in many analytical laboratories but may need modification to accommodate small sample sizes – typically with addition of a microscope optically coupled to the measurement system. This includes grating spectrometers, in which a broad-band source is passed through slits and onto a grating to select only a narrow band of light, Fourier Transform Spectrometers (schematically shown in Figure 1) and broad-band elipsometers in which polarised light is incident at an angle to the substrate surface and the subsequent reflected beam's polarisation state is measured (see Figure 2). Some systems allow both

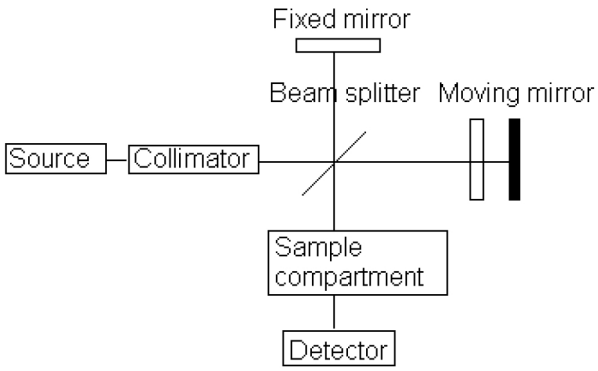


Figure 1: Schematic diagram of a Fourier-transform spectrometer. The interference pattern at the detector is obtained by moving the mirror and changing the optical path length. When a sample is present the interfence pattern, as a function of path difference, is modulated by the presence of absorption bands in the sample. The interference pattern is then 'Fourier transformed' to give the absorption (or reflection/transmission) as a function of wave number to give a spectrum [15].

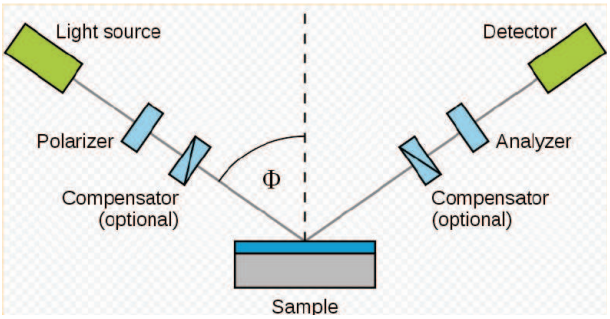


Figure 2: Schematic representation of an elipsometer [16].

transmission and reflection measurements by simple reconfiguration, elipsometers typically allow the angle of incidence to be varied. However, most commercial spectrometers do not allow the angle of incidence to be varied. Similarly, Time Domain Spectroscopy (TSD) in which the phase angle of the measured quantity is obtained from interference methods are usually custom built systems. A simplified schematic of a TDS is shown below in Figure 3. The illuminating EM radiation is generated by the femtosecond pulses from a Ti Sapphire laser incident on either a crystal converter or optoelectronic converter to produce for example THz radiation. The optical delay line alters the phase of the beam arriving at the sample. A detailed introduction is given in reference [17].

## 1.3 Instrumental limitations

At optical frequencies, it is very difficult or even impossible with current technology to measure the electric and magnetic field components of the electromagnetic wave directly versus real time as one cannot measure amplitudes and phases within one wavelength. This can be compared to microwaves were there is still room to manoeuvre (within say a few cm). Therefore the frequency-domain techniques are commonly employed. Usually,

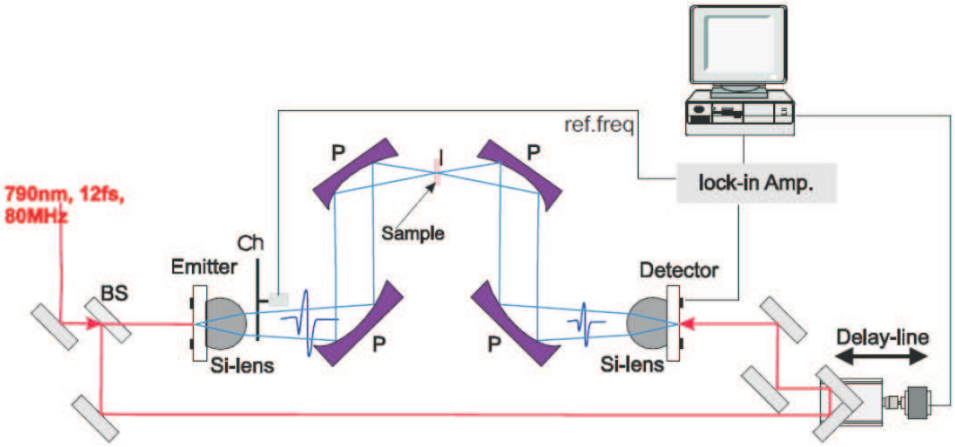


Figure 3: Schematic of Time Domain Spectroscopy [17].

grating spectrometers or Fourier-transform spectrometers merely deliver the intensity of light versus wavelength or frequency. However, all phase information is lost here. Using interferometric techniques, phase information can be (partially) recovered. Commercially available elipsometers promise to deliver optical constants of thin-film samples but in fact measure angle resolved reflectance polarisation data and rely on idealised models to produce optical constants. Extreme caution should be exercised at this point, because the built-in commercial software used for analyzing (or, more precisely, interpreting) these data is limited to dielectric material responses and layered systems only, but it is usually unsuitable at all to deal with magnetic responses (or negative refractive indices). Also, the low symmetry of metamaterial samples can be problematic here too.

Due to the limited lateral footprint of typical samples (because of present fabrication limitations), the incident light wave has to be focused onto the metamaterial samples. If light is not focused, most of the light from the source will illuminate the area surrounding the metamaterial sample. Unless this light is eliminated from the measurement (by for example an iris) the measurement will be swamped by the other materials in the system. Once a lens is introduced, it concentrates the light from the aperture of the lens onto the sample but at the expense of averaging over the half angle from the sample to the lens aperture (defined as the numerical aperture, $NA$). This clearly introduces an undesired spread of the incident wave vector components of light, i.e., the experimental results are effectively averaged over a certain range of incidence angles, obviously leading to obscured data. The impact of that averaging process depends on the specific metamaterial under study. For example, it is quite common to image the samples by means of a microscope. As large spectral bandwidths have to be investigated often, reflective microscope objectives are mandatory in order to avoid chromatic aberrations that would otherwise occur for glass-based lenses. It is well known that such Cassegrain objective lenses essentially cut out the normal incidence contribution and average over a cone of angles of incidence (e.g., between 15° and 30° with respect to the surface normal for a numerical aperture of $NA = 0.5$). Again, the impact of these "artifacts" need to be evaluated for each metamaterial structure separately. A sample that matched the source and detector areas and an arrangement that ensured all the scattered light was collected would constitute an ideal measurement.

Measuring broadband intensity transmittance and reflectance spectra with incident circular polarization of light is far from a trivial task. Broadband linear polarizers are readily available in most spectral ranges and a quarter-wave plate can turn this linear polarization into circular polarization. However, a usual quarter-wave plate has obvious inherent wavelength dependence. At optical and near-infrared frequencies, so-called super-achromatic quarter-wave plates are commercially available. At mid-infrared frequencies, such super-achromatic quarter-wave plates have to be custom-made – this incurs significant cost. Also, these structures can not always be easily integrated into existing (commercial) instrumentation. At THz and microwave frequencies, such super-achromatic quarter-wave plates are presently not available at all, to our knowledge.

## 1.4 Recent advances in measurement techniques

Although no new fundamental changes in the ways how metamaterials are measured have been discovered yet, the new developments and refinements in S-parameter measurement techniques have been reported recently, particularly in relation to the phase measurements across the spectrum from visible to microwave region.

- An experimental method implemented in [18] is based upon a white-light Fourier-transform spectral interferometer for broadband 1.1 to 1.7 $\mu$m phase measurements to determine the dispersion relation of metamaterials at normal incidence in terms of the complex wavenumber leading to retrieval of an effective refractive index. The experimental setup is a Jamin-Lebedeff interferometer modified for measurements in transmission and reflection under normal incidence. With this technique an inaccuracy of the refractive-index of about 4% in the real and imaginary parts can be achieved.

  The measurements were performed with a supercontinuum light source (spectral bandwidth 0.4 $\mu$m – 1.7 $\mu$m). After a collimator and a polarizer, the linear polarized light passes a calcite beam displacer, where the beam is divided into two parallel, orthogonally polarized beams with a displacement of 4 mm. These two beams represent the two arms of the interferometer. In the configuration for the transmission phase measurements the beams traverse the sample and then pass an achromatic half-wave plate, which rotates the polarization in each beam by 90°. The two beams are recombined in the second beam displacer. As the beams in the interferometer arms are orthogonally polarized, the interference between them can be obtained using another linear polarizer. Finally, the light is collected into a photonic crystal (PhC) single-mode fiber and measured with an optical spectrum analyzer.

- THz-Time Domain Spectroscopy (TDS) normally requires two measurements [19]: one reference waveform measured with the reference of known dielectric properties, and a second measurement through the sample. Because of the relatively clean separation in time between the main transmitted pulse and the first internal reflection, it becomes possible to keep only the first directly transmitted THz pulse. Comparing the ratio and phase change between the sample and reference, the real part and imaginary part of effective refractive index of studied sample can be obtained

simultaneously. A detailed retrieval procedure enables one to extract the negative refractive index of low-loss metamaterials based on THz-TDS measurements [19].

Detecting the phase change of THz wave passed through the metamaterial sample, as well as the corresponding reference, one can obtain the refractive index of studied sample using the presented extraction procedure. The method provides a direct and simple way to probe the real part and imaginary part of refractive index of metamaterials. Its validity has been demonstrated through theoretical simulations on several typical cases.

# 2 State-of-the-art in experimental characterisation of metamaterials

All experiments published to date have been far away from the ideal conceptual arrangements described in Section 1.1. Several different techniques are usually adopted for the experimental characterisation of metamaterials. The typical approaches are overviewed here.

## 2.1 Structures with inversion symmetry along the surface normal

Suppose that the metamaterial structure exhibits inversion symmetry along the surface normal. In this case, at normal incidence, the reflectance and transmittance spectra do not depend on which side of the sample is illuminated. A quite common procedure is to measure intensity transmittance and/or reflectance spectra of a metamaterial slab of thickness $L$ for normal incidence of light and for two relevant (i.e., linearly independent) incident polarizations, either linear or circular. Clearly, these data containing two quantities at each wavelength are insufficient to retrieve uniquely the optical parameters, e.g., the complex refractive index and the complex impedance of the equivalent isotopic slab at each wavelength. Thus, usually, the experimental data are compared with the theoretical calculations for the designed specimen using additional information on the geometrical parameters which are obtained from optical and/or electron micrographs of the metamaterial samples. If sufficiently good agreement between experiment and theory is obtained, one may apply the theory to compensate for missing experimental phase information.

One way of further analyzing/interpreting the experimental data is to model a fictitious slab of thickness $L$ (with or without substrate) that has exactly the same complex reflectance and transmittance spectra as those of the metamaterial specimen. This "retrieval" procedure (see, e.g., review [3] for discussion of selecting the proper branches of non-unique solutions arising in this process) delivers the two complex quantities for the effective refractive index and impedance, or, equivalently, the effective complex dielectric permittivity and magnetic permeability of the slab. While this procedure is fairly well defined and broadly adopted in many laboratories around the world, one should be cautious in interpreting these retrieved quantities. Namely, they do represent the optical properties of the metamaterial slab with thickness $L$ - yet they do not necessarily constitute the "material" properties in the conventional sense. One might be tempted to

take the knowledge from normal optical materials and transfer it to metamaterials. For example, if one followed the retrieval procedure described above for a thin film of silica ($SiO_2$) of thickness $L$, it is clear that the measurements of the same film but of thickness $2L$ would give nearly identical material parameters. This is very often not (!) the case for metamaterial samples. Generally, (near-field optical) interactions between different functional layers of the metamaterial can alter the effective "material parameters". Whether or not this is a significant effect needs to be evaluated for each metamaterial structure under investigation – there is simply no universal answer. Two published experiments at optical frequencies that have addressed this issue [10, 12], and have come to the conclusion that these interaction effects are not too strong for their conditions (both are several layers of double fishnet negative-index metamaterials). A striking counter-example is in ref. [11], where the strong coupling between adjacent layers of split-ring resonators has tremendously altered the properties of a single layer. Yet, the answer to this question also depends on how strongly the layer proximity influences the structure response. For example, it is known from (dielectric) photonic crystals that, for certain aspects (e.g., slow group velocities), the slab thickness exceeding even 100 lattice cells may be insufficient to reproduce the behaviour predicted by the band structure calculations for the fictitious infinite "material".

## 2.2 Structures with no centre of inversion along the surface normal

The situation becomes more complex if the metamaterial structure has no centre of inversion along the propagation direction of light. Still restricting ourselves to normal incidence of light onto the metamaterial slab, the complex transmittance and reflectance spectra are no longer the same for the two opposite directions of incidence. In other words, generally eight different quantities have to be measured at each wavelength – provided that the polarization state of the incident light is conserved in both reflectance and transmittance. Otherwise, the number of independent optical parameters doubles. In case of reciprocal structures (i.e., no static magnetic bias applied and there is no natural magnetic phase), the complex transmittances are strictly identical for both directions of propagation, whereas the respective complex reflectances may differ. This amounts to six parameters at each wavelength. Again, in the published optical experiments, not the full fields but only the corresponding intensities have been measured. As a result, the problem of the effective parameters' retrieval is underdetermined. As discussed in Section 2.1, additional theoretical input is usually used for extracting the effective optical parameters. One possible approach here is to retrieve the two complex impedances for each side of the equivalent slab at opposite directions of incident waves and a single complex refractive index. Alternatively, the complex permittivity and permeability as well as the bi-anisotropy parameter can be retrieved. Experimentally, this has been done in the literature only once so far in [18]. Needless to say that the meaning of these quantities is subject of the same constraints as in Section 2.1, i.e., caution has to be exercised in interpreting these effective quantities as the "material" parameters. They do, however, have a well defined physical meaning for the measured film of thickness $L$. A variant of the latter approach is proposed in [23] to replace the bi-anisotropy parameter by a wave-vector dependence of permittivity and/or permeability.

## 2.3 Interferometric experiments

Additional information can be obtained from normal-incidence interferometric experiments that – at least partly – recover the missing phase information discussed above. Corresponding publications include Refs. [4, 24–26]. These additional inputs provide further sensitive tests of the level of agreement between the experiment and theory. In that sense, they are very important. However, these additional experimental data do not at all change the conceptual issues of Section 2.1.

## 2.4 Oblique incidence

The situation becomes even more complex at oblique incidence of light onto the metamaterial slab. For usual optical materials, generally all optical quantities become tensors of rank three. Only very few experiments on metamaterials at optical frequencies have addressed oblique incidence of light [27, 28]. These papers have just reported the measured transmittance intensity and/or reflectance spectra at different inclination and azimuth angles, but the authors have completely refrained from relating these measurement data to the effective "material" parameters. Theoretical aspects of the respective retrieval procedures are addressed in the literature, see, e.g., [29, 30].

## 2.5 Chiral metamaterials

Lately, progress has been achieved in manufacturing uniaxial chiral metamaterials operating not only at microwave frequencies [31], but also at THz [32] and optical frequencies [33]. Chiral structures are a subclass of bi-anisotropic structures. In bi-anisotropic structures, magnetic-dipole moments can be excited by the electric-field component of the light field and vice versa. In contrast to the general case of bi-anisotropy, where, e.g., the magnetic-dipole moments and the exciting electric field can include any angle, in isotropic chiral media they are parallel. In lossless media this leads to a pure rotation of any incident linear polarization of light, i.e., to optical activity.

Microwave measurements of chirality parameters of natural and artificial chiral materials is a well-established technique. An overview can be found e.g. in [34, Ch. 7]. Transmission-reflection measurements both in free space and in waveguides have been used for this purpose. Small samples (compared with the free-space wavelength) can be measured also using microwave resonators (perturbation analysis is then used to extract the effective parameters). In more recent literature, a detailed theoretical explanation of how the effective parameters can be retrieved from measured data has explicitly been given in Ref. [35].

Recently, corresponding optical experiments have been performed for chiral metamaterial samples. In Refs. [31, 32] effective material parameters have actually been retrieved from the normal-incidence experimental data, while in Ref. [33] different approach was employed.

The results of [31, 32] have also been discussed in a publication aiming at a broad general readership in ref. [36] (also see references cited therein). An interesting aspect of these latest results is that, for sufficiently strong chirality, a negative phase velocity of

light can be obtained even if, in principle, the dielectric permittivity and the magnetic permeability are positive at the same time [37–39].

Provided that phase information is acquired (see above), the measurements can be performed equivalently either with linear or with circular polarization of the incident light. In Ref. [31], phase-sensitive transmittance and reflectance spectra have been taken with linear polarization of the incident light. In Ref. [32], phase sensitive time-resolved data have been Fourier transformed. In both cases, data have to be taken for different linear polarizations as three complex parameters (dielectric permittivity, magnetic permeability, and chirality parameter shall be retrieved). If no phase information is obtained (i.e., only intensity measurements combined with theory), a minimum requirement for meaningful parameter retrieval is that one checks that the two incident circular polarizations of light stay circular (with the same handedness) upon transmission. Furthermore, following the generalized Fresnel coefficients, left-handed circular polarization has to turn into right-handed circular polarization and vice versa in reflection. In other words, circular polarization cross-conversion needs to be small. This is equivalent to stating that the structures must not exhibit additional linear birefringence. This condition has not been fulfilled in Ref. [33], hence a chirality parameter could not be (and has not been) correctly retrieved.

More recent experimental work [40] has attempted to bring the structures of Ref. [31] (albeit with some modifications and simplifications) towards optical frequencies. Here, circular polarization conversion has been negligible and a maximum difference of the circular refractive indices of about 0.34 has been retrieved [40]. This difference is twice the chirality parameter. Both indices, however, have remained positive throughout the entire spectral range. Still, such structures are interesting and relevant as the optical activity obtained is rather broadband (about 100-nm bandwidth at around 1360-nm center wavelength) and many orders of magnitude larger than what is obtained from, e.g., solutions containing chiral sugar molecules [40].

## 2.6 On measurements of the effective refractive index

In order to somewhat justify the use of the effective refractive index, $n$, of metamaterials made of stacked layers of periodic inclusions, convergence of the retrieved value of $n$ when increasing the number of layers has been studied experimentally in [12]. The observed convergence rate of $n$ proved to be consistent with the findings of the theoretical paper [41] based on a similar double-fishnet type negative-index photonic metamaterial design. Ref. [41] reports convergence for four functional layers. However, one should be aware that these quantities are not the fundamental physical parameters at all. Increasing the spacing between adjacent functional layers of the double-fishnet structure will decrease their coupling (see discussion in Section 2.1). As a result, convergence can even be achieved for a single functional layer [42]. Inferring other optical parameters (e.g., permittivity or permeability) from such refraction experiments [12] again requires making reference to the dedicated theoretical models of the measured specimens.

An alternative type of the refraction measurements is based upon the use of prism made of wedge-shaped metamaterial sample (rather than the slabs discussed so far). The direction of the light wave transmitted through such samples generally changes due

to refraction. Measuring the corresponding light deflection angles allows the refractive index to be inferred by applying Snell's law. However, such obtained refractive index is generally differ from the refractive index n usually referred to in connection with the phase velocity of light, $c$, in material being slower by factor $n$ than the vacuum speed of light, $c_0$, i.e., $c = c_0/n$. A brief discussion of this aspect can be found, e.g., in Ref. [43]. The experiments addressing the change in the direction of the Poynting vector (energy flow) have been published [12]. The samples investigated in [12] were fabricated via evaporation of a stack of 21 alternating layers of silver and dielectric (corresponding to 10 lattice cells). Next, holes were drilled using focused-ion-beam (FIB) lithography to obtain a stacked fishnet type structure. Finally, a wedge which forms a prism has been produced, again using FIB lithography. The measured wavelength-dependent changes in beam direction have been compared with the time-domain simulations in CST Microwave Studio. The calculations agree regarding the real part of the refractive index, and the authors have concluded that ten functional layers (lattice cells) suffice for the retrieved effective refractive index to be representative of the value for "bulk" material. However, the same calculations disagree with the experimental data by a factor larger than five for the imaginary part of the refractive index, i.e., the maximal measured figure of merit of about 3 is much smaller than the calculated value of about 20.

# 3 Concluding remarks

Optical metamaterials, because of their typically limited area and number of functional layers, are more easily understood as finite structures with interfaces that define their optical behaviour. This definition is in contrast to a conventional material in which their bulk properties define their optical properties. The retrieved 'material' parameters are the subject of interpretation unless the samples have sufficient extent in the measurement direction to suppress the interface effects. Also the phase information is harder to obtain giving the need for either more sophisticated measuring tools, such as time domain or interference methods, or alternatively, more complex structures, i.e. phase masks made with the metamaterial.

The current challenges and difficulties of characterization of nanostructured materials have been summarised in [45] where the author stated that "... as we near the one hundred year mark since the birth of crystallography, we face a resilient frontier in condensed matter physics: our inability to routinely and robustly determine the structure of complex nanostructured and amorphous materials. Yet what has become clear with the emergence of nanotechnology is that diffraction data alone may not be enough to uniquely solve the structure of nanomaterials". Commenting on the recent paper [46] which presented the approach to determination of the structure of complex nanostructured materials, the author argued that the major challenges arise from the limited information content of the measurement data along with the growing complexity of the models used for data post-processing. Uniqueness of the associated inverse problems is a real issue, as is the availability of good nanostructure solution algorithms. Additional constraints coming from prior knowledge about the system, or additional data sets, from different information sources are required to constrain a unique solution for retrieval of the material parameters. The author of [45] suggests: "We may be relearning lessons from crystallography... These

constraints are just common sense, but place enormous restrictions on the solution space and the efficiency and uniqueness of solutions. Nanostructure solution is much younger than crystallography, but the field is rapidly growing up."

# References


[1] V.M. Shalaev, Nature Photon. 1, 41 (2007).

[2] C.M. Soukoulis, S. Linden, and M. Wegener, Science 315, 47 (2007).

[3] K. Busch, G. von Freymann, S. Linden, S. Mingaleev, L. Tkeshelashvili, and M. Wegener, Phys. Rep. 444, 101 (2007).

[4] S. Zhang, W. Fan, N.C. Panoiu, K.J. Malloy, R.M. Osgood, and S.R.J. Brueck, Phys. Rev. Lett. 95, 137404 (2005).

[5] N. Feth, C. Enkrich, M. Wegener, and S. Linden, Opt. Express 15, 501 (2007)

[6] W. Wu, E. Kim, E. Ponizovskaya, Z. Liu, Z. Yu, N. Fang, Y.R. Shen, A.M. Bratkovsky, W. Tong, C. Sun, X. Zhang, S.-Y. Wang and R.S. Williams, Appl. Phys. A 87, 143 (2007).

[7] Jin Hyoung Lee, Qi Wu, and Wounjhang Park, Metal nanocluster metamaterial fabricated by the colloidal self-assembly, Optics Letters, Vol. 34, Issue 4, pp. 443-445 (2009)

[8] Jonathan A. Fan, Chihhui Wu, Kui Bao, Jiming Bao, Rizia Bardhan, Naomi J. Halas, Vinothan N. Manoharan, Peter Nordlander, Gennady Shvets, Federico Capasso, Self-Assembled Plasmonic Nanoparticle Clusters, Science, Vol. 328. no. 5982, pp. 1135 - 1138, May 2010.

[9] Kristof Lodewijks, Niels Verellen, Willem Van Roy, Gustaaf Borghs, Pol Van Dorpe, Self-assembled hexagonal double fishnets as negative index materials, Preprint arXiv:1010.5138v1, Oct. 2010.

[10] G. Dolling, M. Wegener, and S. Linden, Opt. Lett. 32, 551 (2007).

[11] N. Liu, H. Guo, L. Fu, S. Kaiser, H. Schweizer, and H. Giessen, Nature Mater. 7, 317 (2008).

[12] J. Valentine, S. Zhang, T. Zentgraf, E. Ulin-Avila, D. A. Genov, G. Bartal, X. Zhang, Nature, 455, 376 (2008); doi:10.1038/nature07247.

[13] H. J. Lezec, J.A. Dionne, and H. Atwater, Science 316, 430 (2007).

[14] Nanostructured Metamaterials, Exchange between experts in electromagnetics and materials science, Ed Anne F de Baas, Luxembourg, European Union 2010, ISBN 978-92-79-07563-6

[15] http://en.wikipedia.org/wiki/Fourier_transform_infrared_spectroscopy, consulted 13.10.2010

[16] http://en.wikipedia.org/wiki/File:Ellipsometry_setup.svg, consulted 13.10.2010

[17] Novel Techniques in THz-Time-Domain-Spectroscopy, A comprehensive study of technical improvements to THz-TDS Matthias Hofmann Inaugural-Dissertation Fakultät für Mathematik und Physik der Albert-Ludwigs-Universität Freiburg im Breisgau vorgelegt von Stefan Gorenflo aus Hausen im Wiesental im November 2006 (see Chapter 3).

[18] E. Pshenay-Severin, F. Setzpfandt, C. Helgert, U. Hbner, C. Menzel, A. Chipouline, C. Rockstuhl, A. Tnnermann, F. Lederer, and T. Pertsch J. Opt. Soc. Am. B, 27, No. 4/ pp 660-666 April 2010.

[19] Jiaguang Han, "Probing negative refractive index of metamaterials by terahertz time-domain spectroscopy", Optics Express, 16, no. 2, pp. 1354 - 1364 (2008).

[20] Ugur Cem Hasar "A Generalized Formulation for Permittivity Extraction of Low-to-High-Loss Materials From Transmission Measurement", IEEE Trans. on Microwave Theory and Techniques, 58, 2, pp. 411-418, Feb. 2010.

[21] Ugur Cem Hasar, "Accurate Complex Permittivity Inversion From Measurements of a Sample Partially Filling a Waveguide Aperture", IEEE Trans. on Microwave Theory and Techniques, 58, 2, pp. 451 - 457, Feb. 2010.

[22] M.S. Rill, C. Plet, M. Thiel, I. Staude, G. von Freymann, S. Linden, and M. Wegener, Nature Mater. 7, 543 (2008).

[23] A.R. Bungay, Yu.P. Svirko, and N. Zheludev, Phys. Rev. B 47, 11730 (1993).

[24] V.M. Shalaev, W. Cai, U.K. Chettiar, H. Yuan, A.K. Sarychev, V.P. Drachev, and A.V. Kildishev, Opt. Lett. 30, 3356 (2005).

[25] G. Dolling, C. Enkrich, M. Wegener, C.M. Soukoulis, and S. Linden, Science 312, 892 (2006).

[26] G. Dolling, M. Wegener, C.M. Soukoulis, and S. Linden, Opt. Lett. 32, 53 (2007).

[27] C. Enkrich, M. Wegener, S. Linden, S. Burger, L. Zschiedrich, F. Schmidt, J. Zhou, T. Koschny, and C.M. Soukoulis, Phys. Rev. Lett. 95, 203901 (2005).

[28] G. Dolling, M. Wegener, A. Schädle, S. Burger, S. Linden, Appl.Phys.Lett. 89, 231118 (2006).

[29] R. Marqus, F. Medina, and R. Rafii-El-Idrissi, Phys. Rev. B 65, 144440 (2002).

[30] X. Chen, B.-I. Wu, J.A. Kong, and T.M. Grzegorczyk, Phys. Rev. E 71, 046610 (2005).

[31] E. Plum, J. Zhou, J. Dong, V. A. Fedotov, T. Koschny, C. M. Soukoulis and N. I. Zheludev, Phys. Rev. B 79, 035407 (2009)

[32] S. Zhang, Y.-S. Park, J. Li, X. Lu, W. Zhang, X. Zhang, Phys. Rev. Lett. 102, 023901 (2009)

[33] N. Liu, H. Liu, S. Zhu, and H. Giessen, Nature Photon. 3, 157 (2009)

[34] I.V. Lindell, A.H. Sihvola, S.A. Tretyakov, A.J. Viitanen, Electromagnetic waves in chiral and bi-isotropic media, Norwood, MA: Artech House, 1994.

[35] D.H. Kwon, D. H. Werner, A. V. Kildishev, and V. M. Shalaev, Opt. Express 16, 11822 (2008)

[36] M. Wegener and S. Linden, Physics 2, 3 (2009)

[37] B.V. Bokut', V.V. Gvozdev, A.N. Serdyukov, Special waves in naturally gyrotropic media, *Journal of Applied Spectroscopy,* vol. 34, pp. 701-706, 1981.

[38] S. Tretyakov, I. Nefedov, A. Sihvola, S. Maslovski, C. Simovski, Waves and energy in chiral nihility, *Journal of Electromagnetic Waves and Applications,* vol. 17, no. 5, pp. 695-706, 2003.

[39] J. Pendry, A Chiral route to negative refraction, *Science,* vol. 306, pp. 1353-1955, 2004.

[40] M. Decker, M. Ruther, C. Kriegler, J. Zhou, C. M. Soukoulis, S. Linden, and M. Wegener, Opt. Lett., submitted (2009)

[41] C. Rockstuhl, T. Paul, F. Lederer, T. Pertsch, T. Zentgraf, T. P. Meyrath, and H. Giessen, Phys. Rev. B 77, 035126 (2008)

[42] C.M. Soukoulis et al., unpublished (2008)

[43] M. Wegener, G. Dolling, and S. Linden, Nature Mater. 6, 475 (2007).

[44] A. A. Sukhorukov, Sangwoo Ha, I. V. Shadrivov, D. A. Powell, and Y. S. Kivshar, Opt. Express 17, 3716 (2009)

[45] S.J.L. Billinge, "The nanostructure problem" Physics 3, 25 (2010), DOI: 10.1103/Physics.3.25

[46] M. J. Cliffe, M. T. Dove, D. A. Drabold, and A. L. Goodwin, "Structure Determination of Disordered Materials from Diffraction Data", Phys. Rev. Lett. 104, 125501 (2010)